Optical spectroscopy of *nP* Rydberg states of ^{87}Rb atoms with a 297-nm ultraviolet laser

Bo Li,[1,2] Meng Li,[1,2] Xiaojun Jiang,[1] Jun Qian,[1,*] Xiaolin Li,[1,†] Liang Liu,[1] and Yuzhu Wang[1]

[1]*Key Laboratory for Quantum Optics, Shanghai Institute of Optics and Fine Mechanics,*
Chinese Academy of Sciences, Shanghai 201800, China
[2]*University of Chinese Academy of Sciences, Beijing 100049, China*

We report the measurement of the absolute transition frequencies of ^{87}Rb atoms to the $nP_{1/2}$ ($n = 34$–52) and $nP_{3/2}$ ($n = 34$–90) Rydberg states by performing single-photon Rydberg excitation spectroscopy in a vapor cell. Rydberg transitions were detected by monitoring the transmission of a 780-nm probe beam. Based on the spectroscopic data, we determined the fine-splitting intervals and oscillator-strength ratios of the nP doublets and also extracted the quantum defects and ionization frequency. These results extend the spectroscopic information of the nP Rydberg series, providing basic knowledge for further applications to Rydberg atoms.

I. INTRODUCTION

Rydberg atoms have generated considerable interest with regard to atom-photon interactions [1], quantum information processing [2], nonlinear quantum optics [3], and Rydberg molecules [4,5], owing to their long lifetime and the long range of the Rydberg interaction [6]. Moreover, atomic Rydberg levels are highly sensitive to external fields, owing to their strong polarizability. These properties make them widely applicable to the detection of microwave and terahertz electric fields [7–11]. Spectroscopic analyses of unperturbed Rydberg states are essential in all these contexts.

Excitation energies, quantum defects, and the fine-structure splitting of Rydberg atoms have been intensively studied for decades, both theoretically [12–14] and experimentally [15–18]. Li *et al.* reported the millimeter-wave spectroscopy of the rubidium nS and nD Rydberg series by using the microwave transitions with a superior frequency resolution of the order of 10 kHz [19]. Furthermore, the absolute transition frequencies of ^{87}Rb to the nS and nD Rydberg states have been measured by electromagnetically induced transparency (EIT), to a spectroscopic accuracy within 1 MHz [20]. The spectroscopic information of the nF states has also been acquired through a three-photon excitation scheme [21]. Spectra for the nP ($n = 30$–60) states were obtained in 1979 with an accuracy of approximately 60 MHz by using pulsed ultraviolet (UV) laser excitation [22]. Li *et al.* also performed a spectral measurement of the nP ($n = 27$–34) states with a spectral resolution of 5 MHz [19]. The spectral data of ^{85}Rb $nP_{3/2}$ ($n = 36$–63), which have an isotope shift compared to the ^{87}Rb state [23], are present in Ref. [24]. However, spectral measurements of the nP states, with both a wide range and a high accuracy, had yet to be investigated.

Single-photon excitations to the nP Rydberg states using a continuous-wave (cw) laser have been reported in recent

years, driven by the increasing maturity of high-power fiber lasers and efficient frequency-doubling techniques. Single-photon Rydberg excitations have been applied in experimental observations of local blockade [25,26], Rydberg molecules [27,28], and Rydberg dressing [29,30]. Thoumany *et al.* demonstrated the Rydberg excitation of the $63P$ state in a room-temperature rubidium vapor cell with a frequency-doubled dye laser of 297 nm wavelength [31]. Single-photon Rydberg excitation spectra of cesium $nP_{3/2}$ states ($n = $ 70–100) have been also investigated in detail very recently [32,33].

Herein, we report the single-photon cw Rydberg excitation spectroscopy of ^{87}Rb atoms in a vapor cell for $n = 34$–52 ($nP_{1/2}$) and $n = 34$–90 ($nP_{3/2}$). A high-power and wavelength-tunable UV laser enabled us to observe the Rydberg transitions directly over a wide range of the principal quantum number n. The factors associated with the linewidth of our spectrum and the absolute transition frequency were investigated. The fine-structure intervals, the ionization frequency, and quantum defects were extracted from the absolute transition frequencies. In addition, the oscillator-strength ratios for the nP ($n = 34$–52) states were extracted from the spectra.

II. EXPERIMENTAL APPROACH

The experimental concept is outlined in Fig. 1. A UV laser (297 nm) and a 780 nm laser were used to perform single-photon Rydberg excitations and spectroscopic measurements, respectively. After frequency stabilization of the 780 nm laser to $5S_{1/2}$, $F = 2 \rightarrow 5P_{3/2}$, $F' = 3$ through Doppler-free saturation absorption spectroscopy, we scanned the UV laser over the nP Rydberg states and observed the increase in the transmission of the 780 nm laser, which is proportional to the ratio $\Gamma_{5P_{3/2}}/\Gamma_{nP}$ of the excited-state lifetimes [31]. Absorption spectroscopy, in its common use, is ill suited to the UV laser used in the present study, because the absorption of the UV light is negligibly small as a result of the weak transition-matrix element between the ground state ($5S$) and the Rydberg state (nP). Consequently, our experiment used the so-called

*jqian@siom.ac.cn
†xiaolin_li@siom.ac.cn
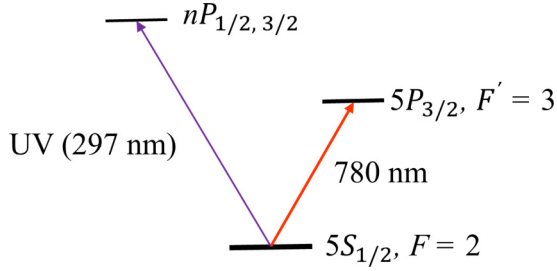
FIG. 1. Energy levels relevant for ^{87}Rb Rydberg spectroscopy. The UV laser excites the atoms from the ground state ($5S$) to the Rydberg state (nP), and the 780-nm laser is used to measure the population change of the $5S$ state following Rydberg excitation.

shelving technique. First introduced by Dehmelt in single-ion experiments [34], it has since been used for the optical detection of weak absorption signals and single-photon Rydberg excitations in particular [31–33]. The experimental setup is depicted in Fig. 2. The UV laser beam was generated using a two-stage frequency-doubling strategy as follows. In the first stage, a seed laser beam (∼50 mW, ∼1188 nm) was sent to a Raman fiber amplifier with a maximum output power of approximately 10 W. Then, the output laser was single-pass frequency doubled to approximately 594 nm (∼2 W) through a PPLN crystal. In the second stage, the 594 nm laser was injected into an optical resonator with a barium borate (BBO) nonlinear crystal to generate a UV laser beam with a maximum power of approximately 200 mW and a wavelength range of 296.9–297.7 nm. The 780 nm laser is frequency locked by means of saturated absorption spectroscopy and split into two beams L1 and L2 on a glass plate. The two beam intensities were equalized using a polarizing beam splitter (PBS). Beam L1 overlapped with the UV laser beam at dichroic mirror M2 and probed the Rydberg excitation. The other beam, L2, served as a reference for balance detection. The $1/e^2$ diameters of the linearly polarized UV and 780 nm laser beams were 1.2 and 1.0 mm, respectively. These beams subsequently copropagated across a 10-cm-long quartz cell filled with Rb vapor (of natural isotopic abundance) and covered with a μ metal shield against stray magnetic fields. The UV beam was modulated by a chopper at 2 kHz. The difference between L1 and L2 beam intensities was measured by a differential photodiode (Newport, 2107-FS) and then amplified by a lock-in amplifier (Stanford Research Systems, SR830) synchronized to the chopper. We chose to record the wavelength of the 594 nm laser as the UV laser is hardly to be coupled into the fiber and could not be directly measured by the wavelength meter (HighFinesse, WS-7). We obtained the frequency of the UV laser by doubling the measured frequency of the 594 nm laser. The 780 nm and 594 nm laser beams were coupled into a wavelength combiner (Thorlabs, NG72F1) connected to the wavelength meter. The wavelength meter was calibrated with the 780 nm laser beam while the frequency of the 594 nm laser beam was monitored. The calibration accuracy was approximately 1 MHz, which was mainly determined by the linewidth of the 780 nm laser (<1 MHz) and the calibration resolution of the wavelength meter (1 MHz). To identify a transmission peak in the Rydberg excitation spectrum, we scanned the frequency of the seed laser by applying a scan voltage to it. Finally, we located the transmission signal with the frequency recorded by the wavelength meter.

III. RESULTS AND DISCUSSIONS

Figure 3 shows a typical single-photon Rydberg excitation spectrum for the 37P Rydberg state. The power of the UV laser beam was fixed at 200 mW. We chose different powers for the probe beams for 37$P_{1/2}$ (50 μW) and 37$P_{3/2}$ (5 μW) to ensure a sufficiently large signal-to-noise ratio (SNR). The fine-structure doublets 37$P_{1/2}$ and 37$P_{3/2}$ were measured separately, given the large fine-splitting interval. We obtained the absolute transition frequency and the linewidth of the
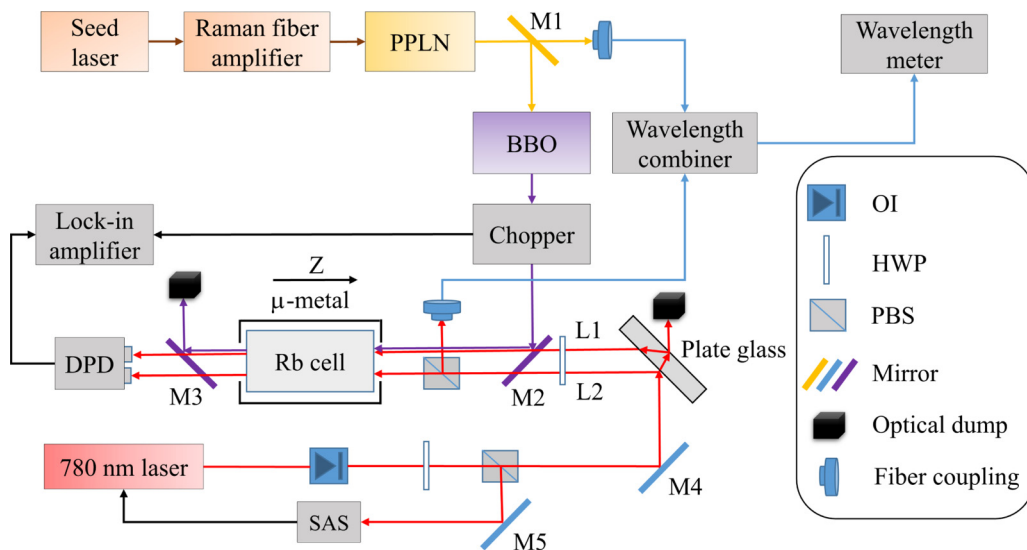
FIG. 2. Experimental setup. PPLN: periodically poled lithium niobate; BBO: beta barium borate; OI: optical isolator; HWP: half-wave plate; PBS: polarizing beam splitter; DPD: differential photodiode; SAS: saturated absorption spectroscopy; M1–M5: mirrors; L1, L2: 780-nm laser beams.
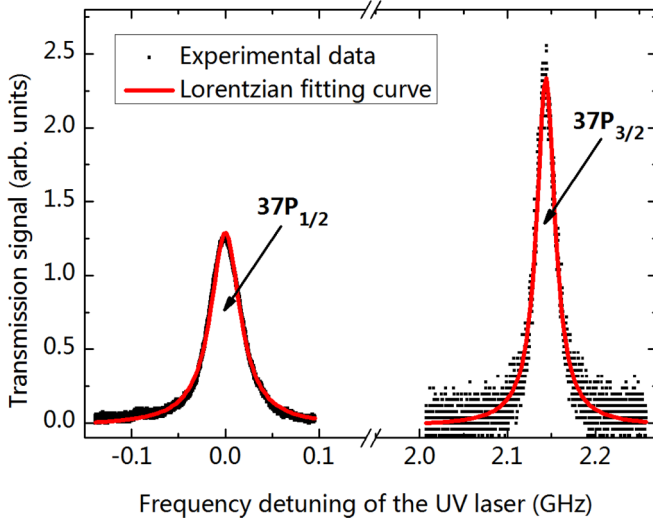
FIG. 3. Single-photon excitation spectra of the Rydberg transitions $5S_{1/2}, F = 2 \rightarrow 37P_{1/2, 3/2}$. The linewidths of the two transmission peaks are 38.7 MHz ($37P_{1/2}$) and 25.4 MHz ($37P_{3/2}$), respectively. The frequency interval between the peaks is 2.14(56) GHz.

transmission peaks by Lorentzian fitting. The absolute transition frequencies of $37P_{1/2}$ and $37P_{3/2}$ are 1007.23334(88) and 1007.23549(44) THz, respectively. The linewidths of the two peaks are 38.0 and 25.4 MHz, respectively.

A. Absolute transition frequency and fine-splitting interval

Following the treatment shown in Fig. 3, we acquired the transition frequencies between the ground state $5S_{1/2}, F = 2$ and the Rydberg states $nP_{1/2}(n = 34–52)$ and $nP_{3/2}(n = 34–90)$, as presented in Tables I and II, respectively. The spectra for $n > 52$ ($nP_{1/2}$) and $n > 90$ ($nP_{3/2}$) were discarded because their mean deviations of several measurements exceeded 5 MHz and did not maintain a stable Lorentzian line shape.

The primary factors that degrade the measurement accuracy of the absolute transition frequency are the frequency instability of the 780 nm laser and the drift of the wavelength meter reading. We obtained the frequency error due to these two factors by observing the frequency drift of the locked 780 nm laser recorded by the wavelength meter. The fre-

TABLE I. Measured absolute transition frequencies between $5S_{1/2}, F = 2$ and $nP_{1/2}(n = 34–52)$ (units in THz). The experimental uncertainty is 5 MHz.

n	Transition frequency	n	Transition frequency	n	Transition frequency
34	1006.6739290	41	1007.7848932	48	1008.4223682
35	1006.8777876	42	1007.8971656	49	1008.4906608
36	1007.0635684	43	1007.0012340	50	1008.5546872
37	1007.2333488	44	1007.0978050	51	1008.6147912
38	1007.3889488	45	1007.1876290	52	1008.6712345
39	1007.5318642	46	1008.2712938		
40	1007.6634426	47	1008.3493898		

TABLE II. Measured absolute transition frequencies between $5S_{1/2}, F = 2$ and $nP_{3/2}(n = 34–90)$ (units in THz). The experimental uncertainty is 5 MHz.

n	Transition frequency	n	Transition frequency	n	Transition frequency
34	1006.6767502	53	1008.7250762	72	1009.3384777
35	1006.8803502	54	1008.7750956	73	1009.3577788
36	1007.0659122	55	1008.8222898	74	1009.3762708
37	1007.2354944	56	1008.8668428	75	1009.3940085
38	1007.3909126	57	1008.9089604	76	1009.4110280
39	1007.5336718	58	1008.9488346	77	1009.4273517
40	1007.6651088	59	1008.9865844	78	1009.4430416
41	1007.7864320	60	1009.0223986	79	1009.4581165
42	1007.8985942	61	1009.0563782	80	1009.4726164
43	1008.0025526	62	1009.0886525	81	1009.4865557
44	1008.0990362	63	1009.1193279	82	1009.4999770
45	1008.1887738	64	1009.1485299	83	1009.5128947
46	1008.2723600	65	1009.1763247	84	1009.5253414
47	1008.3503830	66	1009.2028144	85	1009.5373330
48	1008.4233020	67	1009.2280965	86	1009.5489032
49	1008.4915356	68	1009.2522110	87	1009.5600542
50	1008.5555062	69	1009.2752469	88	1009.5708226
51	1008.6155556	70	1009.2972625	89	1009.5812286
52	1008.6719549	71	1009.3183221	90	1009.5912642

quency variation is lower than 5 MHz over a one-hour period, which is much longer than the time of a single measurement. After placing the cell into the μ-metal shield, the spectral line shift caused by stray magnetic fields (essentially the Earth's magnetic field) was negligible within our measurement accuracy. The stray electric fields, which also produce a spectral line shift, were shielded by ions and electrons on the inner surface of the glass cell [35]. The Autler-Townes splitting, which equals the Rabi frequency of the 780 nm laser (approximately 1.5 and 5 MHz, corresponding to powers of 5 and 50 μW, respectively), can be neglected in our spectrum measurement. Not until the power of the 780 nm laser was increased to about 500 μW did we observe Autler-Townes splitting in the spectrum. The Autler-Townes splitting will degrade the accuracy of the transition frequency and should be avoided in our spectrum measurement. When we measured the Rydberg states, the 780 nm laser power was much lower than 500 μW. Thus no Autler-Townes splitting is expected in our spectrum. Furthermore, the Rydberg interaction, which contributes a spectral line shift and a shape change in the spectrum of a dense Rydberg gas [36], has only a negligible impact in the room-temperature cell. Given the above discussions, the same as the uncertainty expression employed in Refs. [20,24], the experimental uncertainties of the transition frequencies could be expressed with an overall uncertainty of 5 MHz.

The linewidth, which limits the spectral resolution, could be decreased to approximately 25 MHz in our experiment. Doppler broadening was mostly eliminated because the atoms contributing to the spectrum must be able to interact with both the UV and the 780 nm laser. After Doppler-free frequency locking of the 780 nm laser to $5S_{1/2}, F = 2 \rightarrow 5P_{3/2}, F' = 3$, the atoms with a velocity V_z (where z is the propagation direction of the 780 nm laser beam as shown

in Fig. 2) absorb 780 nm photons if V_z lies within the range $R_v \equiv (-\delta_\Gamma \lambda_{780}/2, \delta_\Gamma \lambda_{780}/2)$, where $\delta_\Gamma \approx 6$ MHz is the natural linewidth of $5P_{3/2}$. The atoms in the velocity range R_v become excited to nP Rydberg states with detuning in the range $(-\delta_\Gamma \lambda_{780}/\lambda_{UV}, \delta_\Gamma \lambda_{780}/\lambda_{UV})$, where the ratio $\lambda_{780}/\lambda_{UV} \approx 2.62$ represents the wavelength mismatch factor [31]. Because the natural linewidth of the nP Rydberg states is much smaller than δ_Γ, the minimum full width at half maximum (FWHM) of the spectrum to which these atoms contribute is approximately 15.7 MHz. Atoms with a velocity beyond the velocity range R_v, which may contribute to other velocity-selective spectra with a lower amplitude [32], are not considered here.

In addition to the natural linewidth, the linewidth of the spectrum is influenced by transit-time broadening, pressure broadening, residual Doppler broadening, and power broadening. From the beam size and the atomic temperature, we estimated the transit-time broadening to be less than 1 MHz [38]. We believe that the pressure broadening is less than our frequency uncertainty (5 MHz) as we did not observe a dependence of the linewidth on n [39]. Misalignment of the 780 nm laser and the UV laser can cause a residual Doppler broadening [33]. Except for the power broadening, these broadening mechanisms are irrelevant to the laser power and contribute broadening to the spectrum of the $nP_{1/2}$ and $nP_{3/2}$ states on a similar scale.

The power broadening caused by the 780 nm laser in the measurement of the $nP_{3/2}$ states is considered negligible because we have not observed an obvious change in the linewidth of the $nP_{3/2}$ transmission peaks when reducing the power of the 780 nm laser from 10 μW to 5 μW, but it nonetheless played a significant role during the measurements of the $nP_{1/2}$ states. The small electric-dipole matrix element of the $5S \rightarrow nP_{1/2}$ transition leads to a weak transmission peak that is difficult to distinguish. Thus a greater laser power (780 nm) is required to increase the SNR of the $nP_{1/2}$ peak. On the one hand, the spectral amplitude varies linearly with the Rabi frequency of the 780 nm laser and correlates positively with the Rabi frequency of the UV laser [32]. On the other hand, as a result of power broadening, the linewidth varies as the square of the Rabi frequency of the probe laser (780 nm) [32]. There is thus a trade-off between the SNR and the linewidth. For the $nP_{1/2}$ states, we increased the 780 nm laser power from 5 μW to 50 μW, which is the only experimental condition changed, and observed the linewidth to increase from about 25 MHz to about 38 MHz. Here, the contribution originating from the power broadening can be estimated to be about 13 MHz. With regard to the UV laser, the Rabi frequency is small even for a power of 200 mW, given the weak electric-dipole transition probability. Thus the power broadening caused by the UV laser is considered to be negligible.

The hyperfine structure of the high-lying Rydberg states can be measured using the millimeter-wave transition [19,40] or electromagnetically induced transparency technology [41], and is not resolved in our experiment. According to the hyperfine structure constant [$A = 4.04(3)$ MHz, $B = 0.55(3)$ MHz] shown in Ref. [42], the hyperfine splitting interval between $9P_{3/2}, F = 2$ and $9P_{3/2}, F = 1$ ($A - B$) was approximately 3.49 MHz. Besides, the hyperfine structure has n^{*-3} scaling

TABLE III. Fine-structure interval of the ^{87}Rb nP states with $n =$ 35–52, in units of GHz. The uncertainty is about 7 MHz according to the error propagation formula [37].

n	Fine-structure interval	n	Fine-structure interval	n	Fine-structure interval
34	2.8212	41	1.5388	48	0.9338
35	2.5626	42	1.4286	49	0.8748
36	2.3438	43	1.3186	50	0.8190
37	2.1456	44	1.2312	51	0.7644
38	1.9638	45	1.1448	52	0.7204
39	1.8076	46	1.0662		
40	1.6662	47	0.9932		

of the splitting interval, where n^* is the effective quantum number [19]. Thus the splitting interval became much smaller than the linewidth of our spectrum for $n^* \geqslant 34$. We believe that we have not observed the hyperfine structure under the present experimental conditions.

The fine-splitting interval ν_{fs} is easily extracted from the absolute transition frequency (see Table III):

$$h\nu_{fs} = \frac{R_y}{(n - \delta_{np_{1/2}})^2} - \frac{R_y}{(n - \delta_{np_{3/2}})^2}, \qquad (1)$$

where $R_y = h3289.82119466$ THz [20] is the Rydberg constant and $\delta_{np_{1/2}}$ and $\delta_{np_{3/2}}$ represent the quantum defects of $nP_{1/2}$ and $nP_{3/2}$, respectively. For sufficiently large values of n, the quantum defect can be considered to be constant. We therefore deduce the fine-splitting intervals in the range $n = $ 34–52, with the quantum defects given by Ref. [19], as obtained from the data in the range $n = $ 28–33. The differences between the measurements and the values calculated from Eq. (1) range between -4.5 and 2.5 MHz for the different Rydberg levels (Fig. 4). Given the measurement accuracy of approximately 5 MHz, the values of ν_{fs} agree well with the results derived from the quantum defects in Ref. [19].
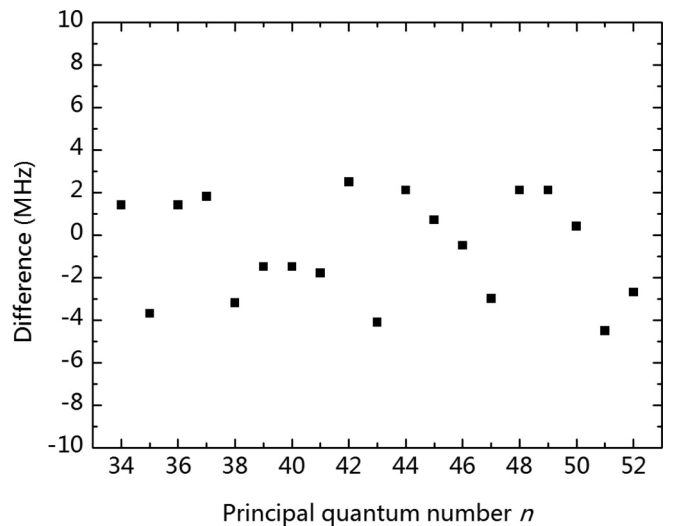
FIG. 4. Difference between the measured fine-splitting interval (see Table III) and the calculated value based on the quantum defects given in Ref. [19].
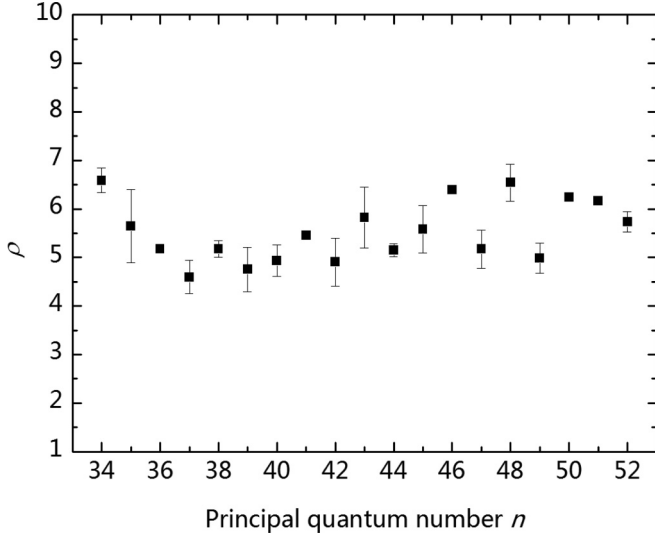
FIG. 5. Oscillator-strength ratio $f_{3/2}/f_{1/2}$ for the Rydberg transitions $5S_{1/2} \rightarrow nP_{3/2}$ and $5S_{1/2} \rightarrow nP_{1/2}$.

B. Oscillator strength ratio

A convenient comparison of the relative transition possibility of the nP fine-structure doublets is given by their oscillator-strength ratio. For the cesium nP states, the ratio are of the order of 10^4 and are difficult to extract [26]. After fixing the powers at 50 μW and 200 mW for the 780 nm laser and the UV laser, respectively, we measured the spectrum of nP ($n = 34$–52) states and extracted the oscillator-strength ratio. The ratio of the oscillator strengths of $nP_{3/2}$ and $nP_{1/2}$, $\rho = f_{3/2,\,5S}/f_{1/2,\,5S}$ ($n = 34$–52), is plotted in Fig. 5. Here, $f_{1/2,\,5S}$ ($f_{3/2,\,5S}$) represents oscillator strengths from the ground state $5S_{1/2}$ to the $nP_{1/2}$ ($nP_{3/2}$) Rydberg states, which can be expressed as [6]

$$ f_{n'l'j'm'_j,nljm_j} = \frac{2m_e}{\hbar} \omega_{n'l'j',nlj} |\langle n'l'j'm'_j|\mathbf{r}|nljm_j\rangle|^2, \quad (2) $$

where $\hbar$ is the reduced Planck constant, m_e is the electron mass, $\omega_{n'l'j',nlj} = (W_{n'l'j'} - W_{nlj})/\hbar$ is the transition frequency, and $|\langle n'l'j'm'_j|\mathbf{r}|nljm_j\rangle|$ is the dipole-matrix element. The value of ρ equals the area ratio of the transmission spectral peaks corresponding to the fine-structure doublets of the nP states [43]. The average oscillator strength is $\rho_{avg} = 5.52 \pm 1.0$, where the uncertainty originates mainly from laser intensity fluctuations.

Various theoretical and experimental works have considered this issue. Previous studies indicate a rising tendency for the ratio as n increases. Thus $\rho = 2$, when measured at a low $n = 5$ [44], increases to $\rho = 4.9 \pm 0.2$ when measured at an intermediate $n = 20$ [45], and plateaus at a constant value as shown in Ref. [22] (5.89 ± 1.4 for $n = 29$–50) and Ref. [43] (4.57 ± 0.46 for $n = 28$–75). We also did not observe a dependence of the oscillator-strength ratio on n within the range $n = 34$–52. This phenomenon is attributed to n-dependent spin-orbit effects and to the core polarizability [46], and also agrees with calculations [47–49]. Our result agrees with the value given in the earlier works, especially the value given by Liberman *et al.* [22].
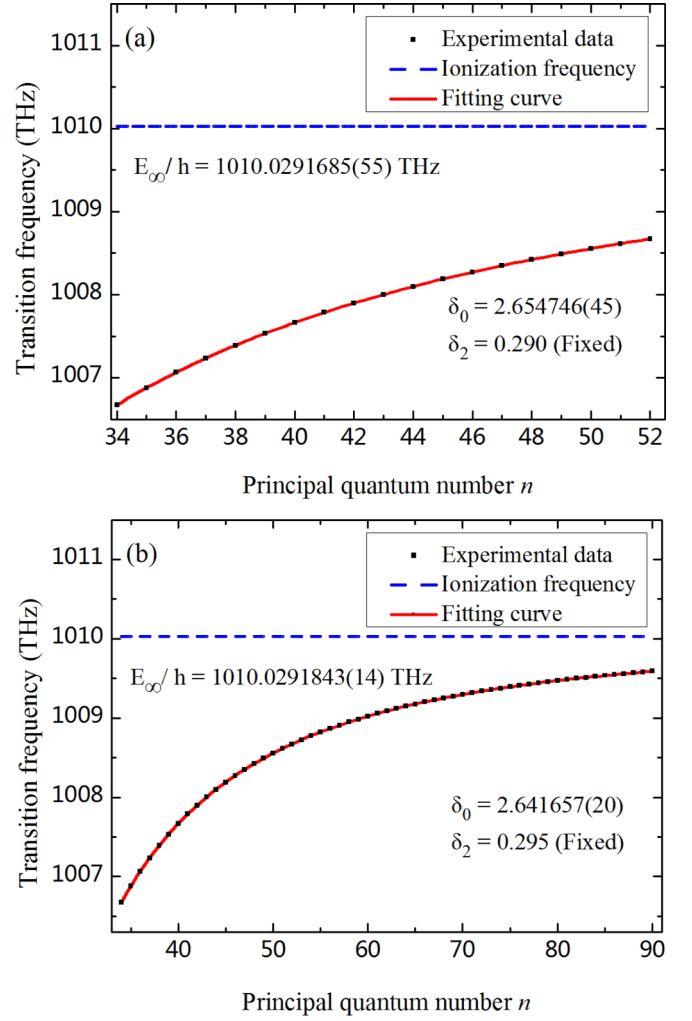
FIG. 6. Fitted curve (red solid line) for the absolute transition frequencies (black squares) of the Rydberg series: (a) $nP_{1/2}$ ($n = 34$–52); (b) $nP_{3/2}$ ($n = 34$–90). The ionization frequency E_∞/h (blue dashed line) and the quantum defects are also specified. The statistical errors are indicated in parentheses.

C. Quantum defect and ionization energy

The quantum defect and ionization energy obey the modified Ritz formula [6]

$$ E_{n,l,j} = E_\infty - E_{hf} - \frac{R_y}{(n - \delta_{n,l,j})^2}, \quad (3) $$

where $E_{n,l,j}$ is the energy of the level described by the quantum numbers n, l, and j, E_∞ is the ionization energy from the ground state $5S_{1/2}$, $F = 1$, $E_{hf} = h6.83468261$ GHz is the hyperfine splitting interval between $5S_{1/2}$, $F = 1$ and $5S_{1/2}$, $F = 2$, $R_y = h3289.82119466$ THz is the Rydberg constant [20], and $\delta_{n,l,j}$ is the quantum defect, which represents an effective change in the value of n arising from the penetration and polarization of the closed inner electron shells. Using the measurements in Tables I and II, we fitted the quantum defects via the expanded formula

$$ \delta_{n,l} = \delta_0 + \frac{\delta_2}{(n - \delta_0)^2} + \frac{\delta_4}{(n - \delta_0)^4} + \cdots. \quad (4) $$

TABLE IV. Ionization frequency E_∞/h from $5S_{1/2}$, $F = 1$ and the quantum defect δ_0 (with δ_2 fixed to 0.29 and 0.295 for $nP_{1/2}$ and $nP_{3/2}$, respectively), as determined in this study. The ionization frequency is taken from Mark *et al.* [20] and the quantum defects from Li *et al.* [19].

		Mark *et al.* [20]	Li *et al.* [19]	This work
δ_0	$nP_{1/2}$		2.6548849 (10)	2.654746(45)
	$nP_{3/2}$		2.6416737 (10)	2.641657(20)
E_∞/h		1010.0291646(3) THz		1010.0291685(55) THz ($nP_{1/2}$)
				1010.0291843(14) THz ($nP_{3/2}$)

When $n > 30$, sufficient accuracy is achieved by fitting only the first two terms on the right side of Eq. (4). To verify the accuracy of the available experimental data, we chose to fix δ_2 to 0.29 ($nP_{1/2}$) and 0.295 ($nP_{3/2}$), as reported in Ref. [19]. Values for δ_0 and E_∞, for $nP_{1/2}$ and $nP_{3/2}$, were deemed acceptable when they minimized the difference between the measured transition frequencies and the transition frequencies calculated with Eqs. (3) and (4). The experimental data and the fit results are shown in Fig. 6. We also present the values of δ_0 and E_∞/h in Table IV, together with those estimated in Refs. [19,20]. The the numbers in the parentheses of our fitting results are the standard error which represents the deviation between the experimental data and the fitting result. Although the quantum defect depends only weakly on n, an additional fitting error is introduced by assuming it to be constant over such a wide range of the principal quantum number ($n = 34$–90). A more precise approach is to perform a piecewise fitting or to fit separately for every state [22]. The ionization energy 1010.0291685(55) THz obtained from the data for ($nP_{1/2}$) ($n = 34$–52) is therefore more reliable than the 1010.0291843(14) THz derived from the data for ($nP_{3/2}$) ($n = 34$–90) and is more consistent with the result given in Ref. [20]. Now, we are in a position to compare our measurements of the ^{87}Rb Rydberg transition frequencies with those of the ^{85}Rb atom in Ref. [24]. Accounting for the ground-state hyperfine structure (4.27167663181518 GHz [50]) and the ground-state isotope shift [164.35(95) MHz [23]], we compared our transition frequencies with the data of $nP_{3/2}$ ($n = 36$–63) given by Sanguinetti *et al.* [24] and found an overall deviation of 39(12) MHz (the number in parentheses is the standard deviation). Similarly, the ionization frequency determined by us differs from the value given by Sanguinetti *et al.* by approximately 33 MHz, which is largely responsible for the overall deviation in the transition frequencies. As shown in Table IV, the ionization frequency we determined is slightly different (approximately 3.9 MHz) from the value given by Mack *et al.* [20], whose frequency uncertainty was lower than 1 MHz.

IV. CONCLUSION

To summarize, we have measured the absolute transition frequencies from the $5S$ to nP Rydberg states of ^{87}Rb in a single-photon excitation scheme. The high-power and wavelength-tunable UV laser allows for the excitation of the $nP_{1/2}$ ($n = 34$–52) and $nP_{3/2}$ ($n = 34$–90) states over a large range of the principal quantum number. The linewidths of the transmission peaks are approximately 39 MHz ($nP_{1/2}$) and 25 MHz ($nP_{3/2}$), which depend primarily on the linewidth of the $5P_{3/2}$ and the power broadening caused by the 780 nm laser. The accuracy of the measured absolute transition frequency (5 MHz) is limited by the frequency instability of the 780 nm laser and the frequency drift of the wavelength meter. We also determined the fine-splitting intervals ($n = 34$–52), the average oscillator-strength ratio ($\rho_{\rm avg} = 5.52 \pm 1.0$), the ionization frequency from the ground state $5S_{1/2}$, $F = 1$ [1010.0291685(55) THz], and the quantum defects for $nP_{1/2}$ [$\delta_0 = 2.654746(45)$ with δ_2 fixed to 0.290] and $nP_{3/2}$ [$\delta_0 = 2.641657(20)$ with δ_2 fixed to 0.295]. The spectroscopic accuracy depends mainly on the frequency stability of the 780 nm laser and the measurement accuracy of the wavelength meter. This can be further improved by locking the 780 nm laser to a reference cavity made of ultralow expansion (ULE) glass and calibrating the wavelength meter with a frequency comb.

[1] S. Haroche and J. M. Raimond, *Exploring the Quantum: Atoms, Cavities, and Photons* (Oxford University Press, Oxford, 2006).

[2] M. Saffman, T. G. Walker, and K. Mølmer, Rev. Mod. Phys. **82**, 2313 (2010).

[3] C. Murray and T. Pohl, *Advances in Atomic, Molecular, and Optical Physics* (Academic Press, New York, 2016), Vol. 65, Chap. 7, pp. 321–372.

[4] W. Li, T. Pohl, J. M. Rost, S. T. Rittenhouse, H. R. Sadeghpour, J. Nipper, B. Butscher, J. B. Balewski, V. Bendkowsky, R. Löw, and T. Pfau, Science **334**, 1110 (2011).

[5] D. Booth, S. T. Rittenhouse, J. Yang, H. R. Sadeghpour, and J. P. Shaffer, Science **348**, 99 (2015).

[6] T. F. Gallagher, *Rydberg Atoms* (Cambridge University Press, Cambridge, UK, 1994).

[7] J. A. Sedlacek, A. Schwettman, H. Kübler, R. löw, T. Pfau, and J. P. Shaffer, Nat. Phys. **8**, 819 (2012).

[8] J. A. Gordon, C. L. Holloway, A. Schwarzkopf, D. A. Anderson, S. Miller, N. Thaicharoen, and G. Raithel, Appl. Phys. Lett. **105**, 024104 (2014).

[9] H. Fan, S. Kumar, J. Sheng, J. P. Shaffer, C. L. Holloway, and J. A. Gordon, Phys. Rev. Appl. **4**, 044015 (2015).

[10] D. A. Anderson, S. A. Miller, G. Raithel, J. A. Gordon, M. L. Butler, and C. L. Holloway, Phys. Rev. Appl. **5**, 034003 (2016).

[11] C. G. Wade, N. Šibalić, N. R. de Melo, J. M. Kondo, C. S. Adams, and K. J. Weatherill, Nat. Photon. **11**, 40 (2017).

[12] L. G. D'yachkov and P. M. Pankratov, J. Phys. B **27**, 461 (1994).

[13] M. Pawlak, N. Moiseyev, and H. R. Sadeghpour, Phys. Rev. A **89**, 042506 (2014).

[14] A. Sanayei, N. Schopohl, J. Grimmel, M. Mack, F. Karlewski, and J. Fortágh, Phys. Rev. A **91**, 032509 (2015).

[15] K. C. Harvey and B. P. Stoicheff, Phys. Rev. Lett. **38**, 537 (1977).

[16] P. Goy, C. Fabre, M. Gross, and S. Haroche, J. Phys. B **13**, 3 (1980).

[17] C.-J. Lorenzen and K. Niemax, Z. Phys. A **315**, 127 (1984).

[18] H. Saßmannshausen, F. Merkt, and J. Deiglmayr, Phys. Rev. A **87**, 032519 (2013).

[19] W. Li, I. Mourachko, M. W. Noel, and T. F. Gallagher, Phys. Rev. A **67**, 052502 (2003).

[20] M. Mack, F. Karlewski, H. Hattermann, S. Höckh, F. Jessen, D. Cano, and J. Fortágh, Phys. Rev. A **83**, 052515 (2011).

[21] L. A. M. Johnson, H. O. Majeed, B. Sanguinetti, T. Becker, and B. T. H. Varcoe, New J. Phys. **12**, 063028 (2010).

[22] S. Liberman and J. Pinard, Phys. Rev. A **20**, 507 (1979).

[23] L. Aldridge, P. L. Gould, and E. E. Eyler, Phys. Rev. A **84**, 034501 (2011).

[24] B. Sanguinetti, H. O. Majeed, M. L. Jones, and B. T. H. Varcoe, J. Phys. B: At., Mol., Opt. Phys. **42**, 165004 (2009).

[25] D. Tong, S. M. Farooqi, J. Stanojevic, S. Krishnan, Y. P. Zhang, R. Côté, E. E. Eyler, and P. L. Gould, Phys. Rev. Lett. **93**, 063001 (2004).

[26] A. M. Hankin, Y.-Y. Jau, L. P. Parazzoli, C. W. Chou, D. J. Armstrong, A. J. Landahl, and G. W. Biedermann, Phys. Rev. A **89**, 033416 (2014).

[27] M. A. Bellos, R. Carollo, J. Banerjee, E. E. Eyler, P. L. Gould, and W. C. Stwalley, Phys. Rev. Lett. **111**, 053001 (2013).

[28] T. Niederprüm, O. Thomas, T. Eichert, C. Lippe, J. Pérez-Ríos, C. H. Greene, and H. Ott, Nat. Commun. **7**, 12820 (2016).

[29] Y.-Y. Jau, A. M. Hankin, T. Keating, I. H. Deutsch, and G. W. Biedermann, Nat. Phys. **12**, 71 (2016).

[30] J. Zeiher, R. van Bijnen, P. Schauß, S. Hild, J.-Y. Choi, T. Pohl, I. Bloch, and C. Gross, Nat. Phys. **12**, 1095 (2016).

[31] P. Thoumany, T. Hänsch, G. Stania, L. Urbonas, and T. Becker, Opt. Lett. **34**, 1621 (2009).

[32] J. Y. Wang, J. D. Bai, J. He, and J. M. Wang, Opt. Express **25**, 22510 (2017).

[33] J. Bai, J. Wang, S. Liu, J. He, and J. Wang, Appl. Phys. B **125**, 33 (2019).

[34] H. Dehmelt, IEEE Trans. Instrum. Meas. **31**, 83 (1982).

[35] A. K. Mohapatra, T. R. Jackson, and C. S. Adams, Phys. Rev. Lett. **98**, 113003 (2007).

[36] C. Carr, R. Ritter, C. G. Wade, C. S. Adams, and K. J. Weatherill, Phys. Rev. Lett. **111**, 113901 (2013).

[37] I. Hughes and T. A. Hase, *Measurements and their Uncertainties: A Practical Guide to Modern Error Analysis* (Oxford University Press, Oxford, 2010).

[38] W. Demtröder, *Laser Spectroscopy: Basic Concepts and Instrumentation* (Springer, Berlin, 1996).

[39] B. P. Stoicheff and E. Weinberger, Phys. Rev. Lett. **44**, 733 (1980).

[40] F. Merkt and A. Osterwalder, Int. Rev. Phys. Chem. **21**, 385 (2002).

[41] A. Tauschinsky, R. Newell, H. B. van Linden van den Heuvell, and R. J. C. Spreeuw, Phys. Rev. A **87**, 042522 (2013).

[42] E. Arimondo, M. Inguscio, and P. Violino, Rev. Mod. Phys. **49**, 31 (1977).

[43] D. Tong, S. M. Farooqi, E. G. M. van Kempen, Z. Pavlovic, J. Stanojevic, R. Côté, E. E. Eyler, and P. L. Gould, Phys. Rev. A **79**, 052509 (2009).

[44] L. N. Shabanova and A. N. Shlyustalov, Opt. Spectrosc. (USSR) **56**, 128 (1984).

[45] E. Caliebe and K. Niemax, J. Phys. B **12**, L45 (1979).

[46] J. C. Weisheit, Phys. Rev. A **5**, 1621 (1972).

[47] J. Migdalek and W. E. Baylis, Can. J. Phys. **57**, 1708 (1979).

[48] J. Migdalek and Y.-K. Kim, J. Phys. B **31**, 1947 (1998).

[49] E. Luc-Koenig and A. Bachelier, J. Phys. (Paris) **39**, 1059 (1978).

[50] S. Bize, Y. Sortais, M. S. Santos, C. Mandache, A. Clairon, and C. Salomon, Europhys. Lett. **45**, 558 (1999).